ARTICLES

Terrestrial nitrogen and noble gases in lunar soils

M. Ozima[1], K. Seki[2], N. Terada[2]†, Y. N. Miura[3], F. A. Podosek[4] & H. Shinagawa[2]†

The nitrogen in lunar soils is correlated to the surface and therefore clearly implanted from outside. The straightforward interpretation is that the nitrogen is implanted by the solar wind, but this explanation has difficulties accounting for both the abundance of nitrogen and a variation of the order of 30 per cent in the $^{15}N/^{14}N$ ratio. Here we propose that most of the nitrogen and some of the other volatile elements in lunar soils may actually have come from the Earth's atmosphere rather than the solar wind. We infer that this hypothesis is quantitatively reasonable if the escape of atmospheric gases, and implantation into lunar soil grains, occurred at a time when the Earth had essentially no geomagnetic field. Thus, evidence preserved in lunar soils might be useful in constraining when the geomagnetic field first appeared. This hypothesis could be tested by examination of lunar farside soils, which should lack the terrestrial component.

Since the Apollo missions, it has been recognized that the Moon is very strongly depleted in volatile elements, including N, H, C and the noble gases[1,2]. The inventory of these elements in lunar materials is not intrinsically lunar but rather reflects an extralunar origin. The extralunar source is generally understood to be the Sun, via direct implantation of solar wind (SW) ions in the surface of the Moon. This interpretation suffices well for the other volatile elements, but encounters difficulty with N—that is, there is too much N compared to the canonical solar abundance (of, for example, Ar), and the isotopic composition ($^{15}N/^{14}N$) of surface-correlated and presumably extralunar N is strongly variable, by as much as 30%. The overabundance of N has been attributed to underabundance of noble gases such as Ar (refs 1, 2), and the isotopic variation to the variation of N composition in the source region of the SW.

However, quantitative evaluations[3] preclude any suggested mechanism by which the isotopic composition of N could vary so much in either the photosphere or the SW. This has led in turn to hypotheses in which some or most surface-correlated lunar N is extrasolar as well as extralunar: that is, it reflects a source other than the SW. Potential sources that have been suggested include interstellar gas, intrinsic lunar N degassed from the interior, the terrestrial atmosphere and infall of cometary or asteroidal debris. The extrasolar interpretation has been strengthened by recent experimental results[4,5]. Overall, no specific model has gained a clear ascendancy.

Here we propose that sources of the extrasolar N and light noble gases in lunar soils can be attributed to ion flows from the atmosphere of a non-magnetic Earth. Mechanisms responsible for the atmospheric escape from a planet depend on its magnetic field[6,7]. An atmospheric source of extrasolar N in lunar soils was suggested in a framework of ion implantation in Earth's magnetotail[3,8]. However, recent observations of the O^+ escape flux[7] and the N^+/O^+ ratio[9] indicate that the N^+ flux at the Moon is less than $10^3\,cm^{-2}\,s^{-1}$, which is insufficient to account for the extrasolar N flux in lunar soils. However, if the geomagnetic field (GMF) were absent, the SW would directly interact with the upper atmosphere, causing a much larger ion escape flux.

The origin of the GMF is still not well understood; in particular, the fundamental issue of when it first appeared remains enigmatic. The oldest palaeomagnetic information available is based on palaeointensity measurements on the Komati formation (age 3.5 Gyr)[10], which showed a much smaller virtual geomagnetic dipole moment than the present value. (But also note that this conclusion is not unchallenged[11].)

If the origin of the GMF were concomitant with the formation of a liquid core, the age of the appearance of the GMF would probably be essentially the same as that of the Earth, earlier than the formation of any significant fraction of the present regolith. For such an early appearance of the GMF, we could thus not expect preservation of any record in lunar soils. On the other hand, if the appearance of the GMF were significantly delayed, it is possible that there was a significant window when the Earth had no GMF and the Moon had a stable regolith surface that could preserve implanted ions to the present day. In that case, the onset of the geomagnetic dynamo might be recorded in lunar soils.

Ion escape from a non-magnetic Earth

In the presence of the GMF, the SW approaching the Earth is stopped at the magnetopause (at a distance of ~10 Earth radii, $10R_E$), where the GMF magnetic pressure balances the SW dynamic pressure. If the GMF did not exist or were much weaker, the SW would approach much closer to the Earth, until its dynamic pressure was balanced by ion pressure at the ionopause, about 500 km above the surface. The SW must thus have interacted directly with the ionized (by solar radiation) upper atmosphere. Atmospheric ions around the ionopause could then have been picked up by the incoming SW and carried away from the Earth[6]. This SW-induced ion escape mechanism from a non-magnetic planet has been observed for Venus[12], which has no permanent magnetic dipole. Thus, if the GMF were absent or extremely weak, we would expect substantial ion escape from the Earth's ionosphere. Some fraction of the escaping ions would have hit the Moon.

Pioneer Venus Orbiter (PVO) observed an escape flux of $\sim 5 \times 10^7\,O^+$ ions $cm^{-2}\,s^{-1}$ from the venusian atmosphere[12], and $N^+/O^+ \approx 0.02$ at the ionopause[13]. The escape of low-energy

[1]Graduate School of Earth and Planetary Science, University of Tokyo, Tokyo 113-0033, Japan. [2]Solar-Terrestrial Environment Laboratory, Nagoya University, Honohara 3-13, Toyokawa, Aichi 442-8507, Japan. [3]Earthquake Research Institute, University of Tokyo, Tokyo 113-0032, Japan. [4]Institute of Isotope Geology and Mineral Resources, ETH-Zentrum, 8092 Zürich, Switzerland, and Department of Earth Planetary Sciences, Washington University, St Louis, Missouri 63130-4893, USA. †Present address: National Institute of Information and Communications Technology, Tokyo 184-8795, Japan.

ions through the iontail suggests a magnetohydrodynamic type of ion outflow, independent of the ion mass, and we infer an N^+ escape flux of 10^6 ions $cm^{-2}\,s^{-1}$ from the venusian atmosphere. It is commonly assumed that the major constituent of the primitive Earth's atmosphere (before the growth of biogenic O) was CO_2 (ref. 14). Therefore, if the ancient Earth did not have a GMF, we expect an escape flux of N from the ancient Earth similar to that from Venus.

To examine ion escape fluxes from a non-magnetic Earth quantitatively, we have made numerical calculations to estimate ion escape fluxes of N^+ and the light noble gases He^+, Ne^+ and Ar^+ from a presumed non-magnetic Earth. These calculations were made for the present Earth's upper atmosphere from the MSIS00 model[15], with the ion production rate given by ref. 16. We assume that all ions produced above the ionopause are picked up by the SW and escape. Fluxes were calculated by integrating the total ion production rate over the dayside Earth surface area above the ionopause, normalized by assuming a circular escape area of radius $2R_E$ (see below). Figure 1 shows thus-calculated ion escape rates against ionopause altitude (and corresponding SW dynamic pressure, P_{SW}). If we assume the ionopause altitude of 500 km, which is inferred for a non-magnetic Earth under typical present SW conditions, the calculated ion escape rates for N^+ will be $\sim 10^6$ ions $cm^{-2}\,s^{-1}$ (Fig. 1).

This calculated N^+ escape rate is comparable with the N^+ escape flux ($\sim 10^6$ ions $cm^{-2}\,s^{-1}$) inferred from the PVO. Figure 1 also shows that if the SW dynamic pressure changes from 3.5 to 22 nPa, the ionopause altitude decreases from ~550 km down to ~250 km, and accordingly the ion escape rates, especially of heavy ions such as Ne^+ and Ar^+, undergo drastic increase. For example, the escape rate of N^+ increases from 4×10^5 to 2×10^8, Ne^+ from 60 to 6×10^4, and $^{36}Ar^+$ from 0.004 to 6×10^2 ions $cm^{-2}\,s^{-1}$, respectively. The ion escape flux depends on the scale height of each ion species and increases nearly exponentially with the ionopause altitude, but not with P_{SW}. As the ionopause altitude becomes lower, higher P_{SW} is needed to further decrease the ionopause altitude, as labelled at the right-hand side in the figure, which is based on the altitude profile of the ionospheric pressure.

If the activity of a young Sun were higher than at present and continuous flare events enhanced SW dynamic pressure, the escape rate would have been much higher than the above estimation based on the present Earth's condition. It is also worth noting that the primitive Earth's atmosphere must have been considerably depleted in oxygen relative to the present Earth's atmosphere, which should have brought the ionopause closer to the Earth to increase the ion escape rate. We show below (Table 1 and discussions) that the origin of non-solar components of N and light noble gases in lunar soils can reasonably be attributed to the Earth's ionosphere.

Assuming an N^+ escape flux of 10^6 ions $cm^{-2}\,s^{-1}$ from the Earth, we next estimate the fraction of the escaping ions that will hit the lunar surface. In analogy to the PVO observation, we assumed a circular cross-section of $2R_E$ for the escaping area of terrestrial ions (hereafter Earth wind or EW). In evaluating the probability of the Moon's passage through the EW area, we also considered the variation of the Earth–Moon distance with time; the distance between the Earth and the Moon has been increasing owing to tidal dissipation since the formation of the Earth–Moon system[17,18]. Figure 2a shows a recent estimation of the time variation of the E–M distance[18]. For an Earth–Moon distance of $40R_E$, corresponding to about 4 Gyr ago (Fig. 2a), we infer from Fig. 2b that on average about 0.3% of the EW flux would hit the lunar surface, that is, about 3×10^3 N^+ $cm^{-2}\,s^{-1}$. The N^+ ions will then be implanted in lunar soils with the same velocity as that of the shocked SW of ~ 440 km s^{-1} (~ 1 keV per a.m.u.). As will be shown later (Table 1), the above estimated average N flux (about 3×10^3 atoms $cm^{-2}\,s^{-1}$) that could be transported to the Moon from a non-magnetic Earth is close to the non-solar N flux observed at the lunar surface ($> 2 \times 10^3$ atoms $cm^{-2}\,s^{-1}$).

Non-solar components in lunar soils

Nitrogen. Hashizume *et al.*[19] argued that the isotopic variation in surface-correlated lunar N can best be attributed to the mixing of two distinct components, solar (SW) and a putative planetary

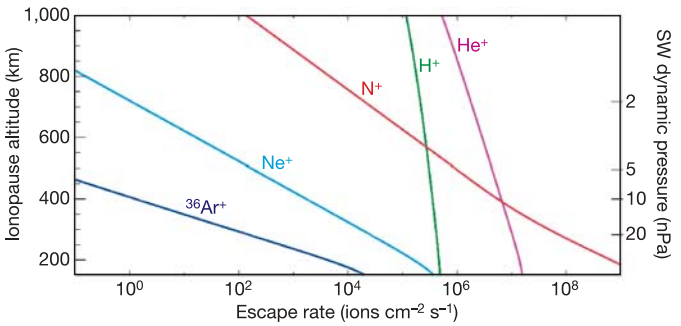

Figure 1 | Ion escape rates versus ionopause altitude for the present Earth's atmosphere without a global magnetic field. Escape rates of $^{36}Ar^+$ (blue), Ne^+ (light blue), N^+ (red), He^+ (magenta) and H^+ (green) ions were estimated using the NRLMSISE00 model of the present Earth's upper neutral atmosphere[15] and ionization rates[16] for normal extreme-ultraviolet flux ($F_{10.7} = 150 \times 10^{-22}$ J $s^{-1}\,m^{-2}$ Hz^{-1}). The ordinate represents both the ionopause altitude (left) and the corresponding solar wind (SW) dynamic pressure (right) derived from the IRI model[32].

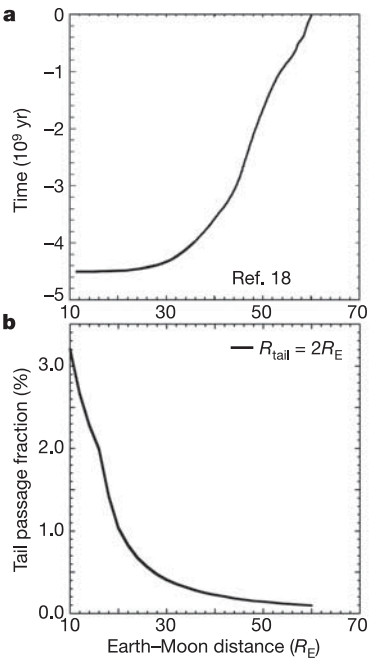

Figure 2 | Estimation of the fraction of the Earth wind (EW) that reaches the Moon. **a**, Earth–Moon distance (in units of Earth radius, R_E) versus age (redrawn from ref. 18); the present day is at time zero. **b**, The time that the Moon spends within the EW tail as a function of the Earth–Moon distance (abscissa). In the ecliptic (x–y) plane, the probability P_{x-y} of the EW tail shadowing the Moon is $\sin^{-1}(S/R)/2\pi$, where R is the distance between the Earth and the Moon, and S is the radius of the EW tail. In estimating the probability P_z of the tail shadowing the Moon in the z-direction, we assume that the Moon's orbital plane is inclined to the ecliptic by $i = 6.7°$ (the present value). Probability P_z then becomes $P(|R\sin(i)\cos(x{:}0 \le x < 2\pi)| < S)$. For the EW flux, we assume a circular cylinder of $2R_E$ radius, as suggested by PVO observation. The total probability $P = P_{x-y} \times P_z$ is shown as a function of R (see **a**). The kink in the curve at $\sim 17R_E$ corresponds to the distance where the lunar orbit starts to exit from the cylindrical EW tail.

Table 1 | SW and EW fluxes in lunar soils

	Solar abundance at Moon surface	SW flux ($cm^{-2}s^{-1}$)	Non-solar comp. (fraction)	Non-solar flux ($cm^{-2}s^{-1}$)	EW flux (estimated) ($cm^{-2}s^{-1}$)	EW flux (calculated) ($cm^{-2}s^{-1}$)
^{4}He	1.0	6.3×10^{6}	~0.3	2×10^{6}	6.7×10^{8}	2×10^{7}
^{20}Ne	1.54×10^{-3}	9.7×10^{3}	~0.3	3×10^{3}	1.0×10^{6}	10^{5}
^{36}Ar	3.27×10^{-5}	206	~0.05	10	3.3×10^{3}	10^{3}
^{14}N*		4×10^{3}	>0.5	2×10^{3}	$>7\times10^{5}$	10^{8}

SW ^{4}He flux at Moon surface (Al foil observation) = 6.3×10^{6} $cm^{-2}s^{-1}$ (ref. 21). Column 1, SW relative elemental (X) abundance at Moon surface = [X]/[^{4}He] (ref. 33). Column 2, SW flux (element X) at Moon surface = [0] × [1]. Column 3, Fraction of non-solar component (X) in lunar soil estimated from a mixing diagram (Figs 3 and 4). Column 4, Non-solar X flux in lunar soil = [2] × [3]. Column 5, Earth Wind (EW) flux = [4]/0.003, if non-solar X were totally attributed to EW (see text). Column 6, EW flux calculated for potential palaeoatmosphere. The height of ionopause is assumed to be 250 km.
*Data for N are from refs 5, 19.

component that they assigned to interplanetary dust particles (IDPs) (Fig. 3). However, other than isotopically this putative IDP component is not well constrained. It may be noted that the N and H isotopic compositions of the assumed planetary component are close to the terrestrial atmospheric compositions, so that the mixing trend suggested in Fig. 3 might be equally well attributed to mixing between SW and terrestrial components.

Light noble gases. If a substantial amount of N can escape from a non-magnetic Earth, we would expect that other volatile elements also escape from the ionopause. Recent experimental observations on light noble gases (He, Ne, Ar) in lunar soils suggest this possibility: Heber *et al.*[20] analysed ilmenite separates (grain ensembles, but not single grains) from Apollo lunar soils (71501, 12001, 74241) and regolith breccias (79135, 79035, 14301) for light noble gases. They found that the isotopic compositions of He, Ne and Ar show significant variation, but also that they are well correlated with each other. As they further pointed out, the correlation clearly indicates that variation in He isotopic ratio cannot be attributed to nuclear process in the Sun, as is often suggested in the literature, since no nuclear process in the Sun can quantitatively affect Ne isotopic ratios. Heber *et al.*[20] therefore suggested that the good correlation between isotopic ratios was due to some experimental artefact. However, we suggest that the observed correlation, not only between ^{3}He/^{4}He and ^{20}Ne/^{22}Ne, but also between ^{3}He/^{4}He and ^{40}Ar/^{36}Ar (the latter correlation was also reported by Geiss[21] for bulk regolith samples) can be well explained on the basis of mixing between SW components and terrestrial atmospheric components.

In Fig. 4a, average ^{3}He/^{4}He and ^{20}Ne/^{22}Ne ratios obtained by Heber *et al.*[20] on six lunar ilmenite separates are reproduced. The data points can be adequately represented by a mixing curve between SW and terrestrial components, where the mixing curve is constructed with three independently estimated mixing parameters and for ionopause altitudes of 500 km, 350 km (shown only for the He-Ne

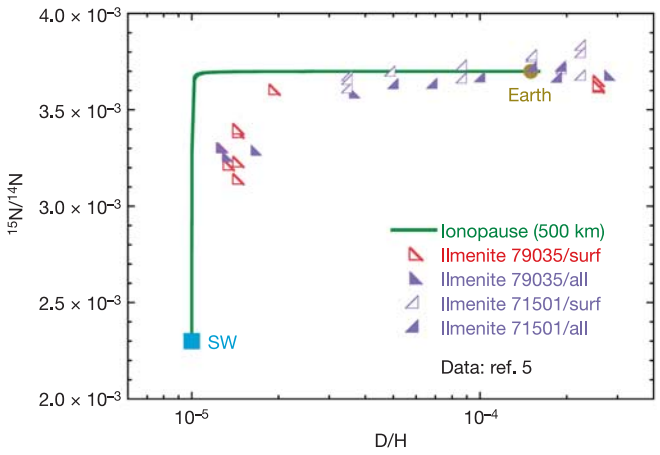

Figure 3 | D/H–^{15}N/^{14}N mixing diagram. Experimental data (red and purple triangles) for individual ilmenite grains separated from Apollo17 breccias (79035 and 71501) obtained in ref. 5 are plotted in a ^{15}N/^{14}N–D/H diagram ('/surf' indicates grain surface; '/all' indicates whole grain). A mixing curve between a SW component (blue square) and a terrestrial component (olive circle) was constructed with three independently estimated parameters (two end member isotopic compositions and the ratio of elemental ratios of the two end members, that is, $r = (^{14}N/H)_E/(^{14}N/H)_{SW}$). We followed refs 5 and 19 for the SW composition. For terrestrial components, we used the present atmospheric ratios, D/H = 1.5×10^{-4} and ^{15}N/^{14}N = 3.7×10^{-3}. The mixing curve is for ionopause height 500 km (but is indistinguishable from the case for 300 km). A ratio of $(^{14}N/H)_E$ (at 500 km) is calculated from Fig. 1.

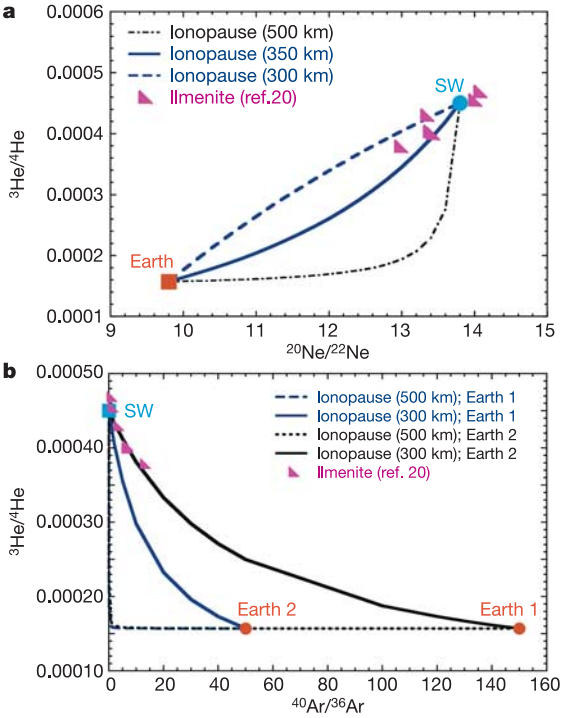

Figure 4 | Mixing diagrams. Shown are mixing diagrams between ^{3}He/^{4}He and ^{20}Ne/^{22}Ne (**a**), and between ^{3}He/^{4}He and ^{40}Ar/^{36}Ar (**b**). Data (filled triangles) are obtained for ilmenite grain ensemble separated from lunar soils (12001, 71501, 74241) and from lunar breccias (14301, 79135, 79035) (ref. 20). **a**, For the SW component (blue circle), we choose the generally assumed values[33] of ^{3}He/^{4}He = 4.5×10^{-4}, ^{20}Ne/^{22}Ne = 13.8 and ^{22}Ne/^{4}He = 1.12×10^{-4}. For the Earth components (orange square), we use the present atmospheric ratio (^{20}Ne/^{22}Ne = 9.8) and the primordial solar ratio (^{3}He/^{4}He = 1.57×10^{-4}; see text). Mixing curves were constructed for ionopause altitudes 500 km, 350 km and 300 km with respective $(^{22}Ne/^{4}He)_E$ ratios estimated from Fig. 1. **b**, For the SW component (blue square), we choose the generally assumed values[32] of ^{3}He/^{4}He = 4.5×10^{-4}, ^{40}Ar/^{36}Ar = 10^{-4} and ^{36}Ar/^{4}He = 3.27×10^{-5}. For the Earth components (orange circles), we assumed ^{3}He/^{4}He = 1.57×10^{-4} for the primordial terrestrial ratio (see text). We constructed mixing curves for ^{40}Ar/^{36}Ar = 50 (Earth 2) and ^{40}Ar/^{36}Ar = 150 (Earth 1), and for ionopause altitudes of 500 km and 300 km, with respective $(^{36}Ar/^{4}He)_E$ ratios calculated from Fig. 1.

case) and 300 km (see Fig. 4 legend). Among the three mixing parameters, the choice of $^3He/^4He$ for the ancient atmosphere deserves special attention, since there are two prominent He components in the early Solar System, namely pre-D-burning He ($^3He/^4He = 1.4 \times 10^{-4}$) and post-D-burning He ($^3He/^4He = 4.5 \times 10^{-4}$). The former is observed in Jupiter's atmosphere[22] and also in the so-called Q component[23] in primitive meteorites. The latter represents He in the present SW (it differs from the primordial value because of creation of ^3He by nuclear 'burning' of D in the pre-main-sequence proto-Sun) and is also observed in some meteorites[24]. From a visual inspection of the mixing diagrams, we note that if the distribution were due to the mixing of the SW and the Earth components, the pre-D-burning He can fairly well be assigned as the Earth end member.

In constructing a mixing curve between SW and terrestrial components for He–Ar, we therefore tentatively used the solar isotopic ratios for SW ($^3He/^4He = 4.5 \times 10^{-4}$ and $^{40}Ar/^{36}Ar = 10^{-4}$) and the pre-D-burning He isotopic ratio for the primitive Earth. However, the choice of appropriate $^{40}Ar/^{36}Ar$ for the ancient Earth atmosphere is difficult because of the extremely rapid evolution in this ratio in the terrestrial atmosphere owing to the addition of radiogenic ^{40}Ar (ref. 25). (For example, the present atmospheric $^{40}Ar/^{36}Ar$ (295.5) is more than six orders of magnitude larger than the primordial cosmic ratio (10^{-4})). We examined mixing curves for two cases, that is, $(^{40}Ar/^{36}Ar)_E = 50$ and 150; here subscript E indicates Earth.

Both He–Ne and He–Ar mixing curves (Fig. 4a, b) appear to show that the pre-D-burning He may be assigned to the end member corresponding to the Earth. A straightforward implication would then be that the Earth inherited the pre-D-burning He when it formed. However, this interpretation requires that the contribution of radiogenic ^4He had not been important in the first 0.5 Gyr or so of the period in which ilmenite grains were likely to be implanted by the EW (see below for the estimation of the SW exposure age). If $U(Th)/^3He$ were large in the Earth, the primordial post-D-burning He might have evolved to the isotopic ratio assumed for the Earth in the mixing diagrams. From the mixing diagrams alone, we cannot rule out either possibility, that is, pre-D-burning or the post-D-burning He as possible primordial He in the Earth.

Implanted EW components

Table 1 shows non-solar N and light noble gas fluxes estimated in lunar soils (details of estimation procedures are also given). From a comparison with curves for various ions (Fig. 1) for an ionopause altitude of 250 km, which is reasonable to assume for the primitive abiogenic atmosphere, we infer that EW can account for non-solar N and Ar (assuming $^{40}Ar/^{36}Ar = 150$) and barely for Ne (about 10%). If the SW flux in ancient times was more intense, which is likely, most of the Ne may also be accounted for by EW.

The SW sweeps ions away above the ionopause regardless of their mass, and would not cause isotopic fractionation of its constituents. The pick-up EW ions are quickly accelerated to the speed of the SW, and some are then implanted in lunar soils with the same velocity as that of the SW. Therefore, it would be difficult to discriminate between implanted EW components from SW components on the basis of the depth profile of implantation in lunar soils. Although ions would not undergo isotopic fractionation once picked up by the SW, isotopic compositions of pick-up ions may reflect fractionation that took place below the ionopause.

Lunar soil, a tracer of GMF evolution?

In order to use lunar soil as a tracer of ancient GMF variation, we must know the time when terrestrial atmospheric components were implanted in lunar soils. If we find that the majority of lunar soils older than a certain age were systematically endowed with a disproportionately large fraction of plausible terrestrial components, we may conclude that GMF did not exist before this age.

Several authors have suggested that the $^{40}Ar/^{36}Ar$ ratio may be used as an antiquity parameter for the surface exposure of lunar soil[26]. However, Ozima *et al.*[27] questioned the validity of this method, since the assumed process (degassing from lunar interior and re-implanting in soil) requires an unrealistically large Ar degassing rate from the lunar interior. Relevant information regarding surface exposure age of lunar soils may be obtained by the use of cosmic ray and surface neutron irradiation effects, but this only tells the time during which samples were within a few metres of the surface, not the exposure time of ilmenite grains directly exposed to the SW. Several samples from Apollo 14 and from Apollo 17 have been studied for the relevant cosmic ray and surface neutron irradiation data[26,28]. Although it is difficult to relate the irradiation age of lunar soil to the surface implantation age of an individual ilmenite grain in the soil, the conclusion by Bernatowicz *et al.*[28] may be worth noting: they stated "the extreme case that the irradiation age coincided with the formation age (of minerals in soils) was most easily in accord with the data at hand". Hence, it may be possible that the substantial fractions of ilmenite grains used in this study had a surface implantation age close to 3.8–3.9 Gyr ago, which is generally assigned to the formation age[29,30] of major impact basins from where the Apollo samples were collected. It is then tempting to speculate that the GMF was null or very weak before about 3.9 Gyr ago.

Test of the hypothesis

Observed data so far available in the literature appear to be consistent with our hypothesis on EW implantation in lunar soils. We suggest that a further test of this hypothesis could be effected by comparing N and light noble gas data for lunar soil/breccia samples from the nearside of the Moon with those from the farside. The Moon–Earth dynamic system, once formed, is thought to have become very promptly (within a few tens of Myr) spin-locked owing to tidal interactions[31]. Thus, only the present nearside of the Moon has been facing the Earth throughout most of the history of the system, and so the farside of the Moon should be essentially free from EW material.

Received 16 November 2004; accepted 9 June 2005.

1. Kerridge, J. F. Solar nitrogen: Evidence for a secular increase in the ratio of nitrogen-15 to nitrogen-14. *Science* **188,** 162–164 (1975).
2. Kerridge, J. F. Corpuscular radiation: Evidence from nitrogen isotopes in the lunar regolith. *Rev. Geophys.* **31,** 423–437 (1993).
3. Geiss, J. & Bochsler, P. Nitrogen isotopes in the solar system. *Geochim. Cosmochim. Acta* **46,** 529–548 (1982).
4. Wieler, R., Humbert, F. & Marty, B. Evidence for a predominantly non-solar origin of nitrogen in the lunar regolith revealed by single grain analyses. *Earth Planet. Sci. Lett.* **167,** 47–60 (1999).
5. Hashizume, K., Chaussidon, M., Marty, B. & Robert, F. Solar wind record on the moon: Deciphering presolar from planetary nitrogen. *Science* **290,** 1142–1145 (2000).
6. Shizgal, B. D. & Arkos, G. G. Nonthermal escape of the atmospheres of Venus, Earth, and Mars. *Rev. Geophys.* **34,** 483–505 (1996).
7. Seki, K., Elphic, R. C., Hirahara, M., Terasawa, T. & Mukai, T. On atmospheric loss of oxygen ions from Earth through magnetospheric processes. *Science* **291,** 1939–1941 (2001).
8. Bochsler, P. Solar wind composition from the Moon. *Adv. Space Res.* **14**(6), 161–175 (1994).
9. Mall, U., Christon, S., Kirsch, E. & Gloeckler, G. On the solar cycle dependence of the N^+/O^+ content in the magnetosphere and its relation to atomic N and O in the Earth's exosphere. *Geophys. Res. Lett.* **29,** doi:10.1029/2001GL013957 (2002).
10. Hale, C. J. & Dunlop, D. Evidence for an early Archean geomagnetic field: a paleomagnetic study of the Komati Formation, Barberton Greenstone belt, South Africa. *Geophys. Res. Lett.* **11,** 97–100 (1984).
11. Yoshihara, A. & Hamano, Y. Paleomagnetic constraints on the Archean geomagnetic field intensity obtained from komatiites of the Barberton and Belingwe greenstone belts, South Africa and Zimbabwe. *Precambr. Res.* **131,** 111–142 (2004).
12. Kasprzak, W. T., Grebowsky, J. M. & Niemann, H. B. Superthermal >36-eV ions observed in the near-tail region of Venus by the Pioneer Venus Orbiter Neutral Mass spectrometer. *J. Geophys. Res.* **96,** 11175–11187 (1991).
13. Grebowsky, J. M., Kasprzak, W. T., Hartle, R. E., Mahajan, K. K. & Wagner, T. C. J. Superthermal ions detected in Venus dayside ionosheath, ionopause, and magnetic barrier regions. *J. Geophys. Res.* **98,** 9055–9064 (1993).

14. Abe, Y. Physical state of the very early Earth. *Lithos* **30,** 223–235 (1993).
15. Picone, J. M. *et al.* Enhanced empirical models of the thermosphere. *Phys. Chem. Earth C* **25,** 537–542 (2000).
16. Richards, P. G., Fennelly, J. A. & Torr, D. G. EUVAC: A solar EUV flux model for aeronomic calculations. *J. Geophys. Res.* **99,** 8981–8992 (1994).
17. Bills, B. G. & Ray, R. D. Lunar orbital evolution: A synthesis of recent results. *Geophys. Res. Lett.* **26,** 3045–3048 (1999).
18. Abe, M. & Ooe, M. Tidal history of the Earth-Moon dynamical system before Cambrian age. *J. Geodet. Soc. Jpn* **47,** 514–520 (2001).
19. Hashizume, K., Marty, B. & Wieler, R. Analyses of nitrogen and argon in single lunar grains: towards a quantification of the asteroidal contribution to planetary surface. *Earth Planet. Sci. Lett.* **202,** 201–216 (2002).
20. Heber, V. S., Baur, H. & Wieler, R. Helium in lunar samples analyzed by high-resolution stepwise etching: Implications for the temporal constancy of solar wind isotopic composition. *Astrophys. J.* **597,** 602–614 (2003).
21. Geiss, J. Solar wind composition and implications about the history of the solar system. *Proc. 13th Int. Cosmic Ray Conf.* 3375–3398 (Denver, University of Denver, 1973).
22. Mahaffy, P. R., Donahue, T. M., Atreya, S. K., Owen, T. C. & Niemann, H. B. Galileo probe measurements of D/H and ^{3}He/^{4}He in Jupiter's atmosphere. *Space Sci. Rev.* **84,** 252–263 (1998).
23. Busemann, H., Baur, H. & Wieler, R. Primordial noble gases in "phase Q" in carbonaceous and ordinary chondrites studied by closed-system stepped etching. *Meteorit. Planet. Sci* **35,** 949–973 (2000).
24. Ozima, M. & Podosek, F. A. *Noble Gas Geochemistry* 2nd edn (Cambridge Univ. Press, Cambridge, 2002).
25. Hamano, Y. & Ozima, M. in *Terrestrial Rare Gases* (eds Alexander, E. C. Jr & Ozima, M.) 155–173 (Japan Scientific Societies Press, Tokyo, 1978).
26. Eugster, O., Terribini, D., Polnau, E. & Kramers, J. The antiquity indicator argon-40/argon-36 for lunar surface samples equilibrated by uranium-235-xenon-136 dating. *Meteorit. Planet. Sci* **36,** 1097–1115 (2001).
27. Ozima, M., Miura, Y. N. & Podosek, F. A. Orphan radiogenic noble gases in lunar breccias: Evidence for planetary pollution of the Sun? *Icarus* **170,** 17–23 (2004).
28. Bernatowicz, T., *et al.* The regolith history of 14307. *Proc. Lunar Sci. Conf.* **VIII** 2763–2783, (1978).
29. Megrue, G. H. Spatial distribution of ^{40}Ar/^{36}Ar ages in lunar breccia 14301. *J. Geophys. Res.* **78,** 3216–3221 (1978).
30. Dalrymple, G. B. & Ryder, G. Argon-40/Argon-39 age spectra of Apollo 17 highlands breccia samples by laser step heating and the age of the Serenitatis basin. *J. Geophys. Res.* **101,** 26069–26084 (1996).
31. Murray, C. D. & Dermott, S. F. *Solar System Dynamics* (Cambridge Univ. Press, Cambridge, 1999).
32. Bilitza, D. International Reference Ionosphere 2000. *Radio Sci.* **36,** 261–275 (2001).
33. Wieler, R. in *Reviews in Mineralogy & Geochemistry* Vol. 47 (eds Porcelli, D., Ballentine, C. J. & Wieler, R.) (Geochemical Society, Mineralogical Society of America, Washington DC, 2002).

Acknowledgements We thank B. Marty, D. Stevenson and K. Zahnle for suggestions and comments that improved the manuscript. We owe much to the work of K. Hashizume, V. Heber, and co-workers, which inspired us to undertake this work. This work is supported by the 21st Century Center of Excellence (21CoE) SELIS (Dynamics of Sun-Earth-Life Interactive System) Program of Japan.

Author Contributions K.S. performed atmospheric escape estimation, and N.T. and H.S. ionospheric modelling.

Author Information Reprints and permissions information is available at npg.nature.com/reprintsandpermissions. The authors declare no competing financial interests. Correspondence and requests for materials should be addressed to M.O. (EZZ03651@nifty.ne.jp).